Physics Letters B 704 (2011) 534–540

Contents lists available at SciVerse ScienceDirect

Physics Letters B

www.elsevier.com/locate/physletb

Isospin-violating dark matter in the Sun

Yu Gao [a], Jason Kumar [b,*], Danny Marfatia [c,d]

[a] Department of Physics, University of Oregon, Eugene, OR 97403, USA
[b] Department of Physics and Astronomy, University of Hawai'i, Honolulu, HI 96822, USA
[c] Department of Physics and Astronomy, University of Kansas, Lawrence, KS 66045, USA
[d] Department of Physics, University of Wisconsin, Madison, WI 53706, USA

ARTICLE INFO

Article history:
Received 8 August 2011
Received in revised form 1 September 2011
Accepted 19 September 2011
Available online 22 September 2011
Editor: M. Trodden

ABSTRACT

We consider the prospects for studying spin-independent isospin-violating dark matter–nucleon interactions with neutrinos from dark matter annihilation in the Sun, with a focus on IceCube/DeepCore (IC/DC). If dark matter–nucleon interactions are isospin-violating, IC/DC's reach in the spin-independent cross section may be competitive with current direct detection experiments for a wide range of dark matter masses. We also compare IC/DC's sensitivity to that of next generation argon, germanium, neon and xenon based detectors.

1. Introduction

The IceCube Collaboration has recently completed installation of the DeepCore extension. An updated estimate of IceCube/DeepCore's sensitivity to spin-dependent dark matter–nucleus scattering [1] with 180 days of data indicates that its sensitivity may be much greater than previously expected [2]. It is therefore of interest to also consider IC/DC's sensitivity to spin-independent scattering (see also [3]).

This interest is heightened by recent developments in dark matter model-building, which have emphasized that dark matter couplings to protons and neutrons may be different. In these models of isospin-violating dark matter (IVDM) [4,5], the cross section for dark matter to scatter off any isotope of an element is determined by the relative number of protons and neutrons in that isotope. This realization has been exploited to construct models that can match the data from DAMA [6], CoGeNT [7] and CRESST [8], while remaining consistent with constraints from other dark matter direct detection experiments [9,10]. In particular, if dark matter interactions with neutrons destructively interfere with those with protons at the $\sim 70\%$ level, then much of the low-mass data can be made consistent.

For the case of partial destructive interference, direct detection experiments using materials with a high atomic mass number A can suffer great losses of sensitivity due to the degradation of the usual A^2 coherent scattering enhancement, as well as the fact that high-A materials usually have a large neutron fraction. Conversely, detectors utilizing low-A materials, such as helium, carbon, nitrogen, oxygen and fluorine exhibit less suppressed sensitivity due to destructive interference. Hydrogen has no neutrons to cause destructive interference. A good way to study IVDM may be through neutrino detectors [11,12], which search for the neutrino flux arising from dark matter annihilating in the Sun after capture by elastic scattering from solar nuclei. Since a significant fraction of dark matter captures arise from scattering off low-A nuclei, neutrino detector sensitivity suffers the least suppression as a result of isospin-violating interactions.

Although isospin violation has been used to understand low-mass dark matter data, these lessons generalize to all mass ranges. For dark matter with mass in the 30–5000 GeV range, the detection prospects from leading experiments, such as CDMS-II and XENON100, can be significantly weakened if dark matter interactions violate isospin. While isospin violation also weakens the sensitivity of neutrino detectors, these sensitivities will be much less suppressed than those of direct detection experiments. Among neutrino detectors, IC/DC will have the best sensitivity to dark matter in this mass range, making it worthwhile to consider its prospects, relative to other direct detection experiments, in probing IVDM.

In this Letter, we perform an analysis of IC/DC's sensitivity to the spin-independent cross section on protons $\sigma_{\rm SI}^p$, including the effects of isospin violation.

2. Indirect dark matter detection via neutrinos

Neutrino detectors search for dark matter which is gravitationally captured in the Sun. The dark matter settles to the core and annihilates to Standard Model products, which in turn produce neutrinos. We focus on the most studied case, where dark matter

* Corresponding author.
E-mail address: jkumar@hawaii.edu (J. Kumar).

0370-2693
doi:10.1016/j.physletb.2011.09.078

Table 1
Relative sensitivities to the W^+W^-, $b\bar{b}$ and $\tau^+\tau^-$ channels at IC/DC obtained from the integrated muon event rates for each of these channels. The $\tau^+\tau^-$ channel proves to be most favorable provided it has a sizable branching fraction. Due to b-hadron absorption by the solar medium, a DM mass significantly above the muon energy detector threshold is necessary for the $b\bar{b}$ channel to be visible. Both upward and contained events at IceCube assume a half-year observation time and an optimistic threshold of 70 GeV. Experimental selection cuts are not included in the IceCube contained rate for which we assume a km^3 volume. The effective area for upward events is given in Ref. [17]. For the DeepCore effective volume we adopt the parameterization of Ref. [14].

m_X	IceCube$_{up}$ (> 70 GeV)		IceCube$_{con.}$ (> 70 GeV)		DeepCore (> 35 GeV)	
	$W^+W^-/\tau^+\tau^-$	$b\bar{b}/\tau^+\tau^-$	$W^+W^-/\tau^+\tau^-$	$b\bar{b}/\tau^+\tau^-$	$W^+W^-/\tau^+\tau^-$	$b\bar{b}/\tau^+\tau^-$
70	–	–	–	–	–	4×10^{-3}
82	0	0	0	0	0.30	5×10^{-3}
90	7×10^{-6}	0	1×10^{-4}	0	0.41	8×10^{-3}
100	0.12	0	0.29	0	0.44	0.012
200	0.68	4×10^{-3}	0.49	0.010	0.40	0.044
300	0.57	0.011	0.39	0.031	0.36	0.069
400	0.50	0.019	0.35	0.052	0.33	0.093
500	0.45	0.025	0.33	0.067	0.32	0.11
600	0.42	0.031	0.31	0.083	0.31	0.12
700	0.38	0.039	0.30	0.10	0.29	0.13
800	0.35	0.044	0.28	0.11	0.28	0.14
900	0.35	0.052	0.29	0.12	0.29	0.15
1000	0.32	0.054	0.27	0.12	0.28	0.15
2000	0.27	0.11	0.27	0.19	0.27	0.20
3000	0.26	0.15	0.27	0.21	0.28	0.22
4000	0.22	0.16	0.23	0.21	0.23	0.21
5000	0.41	0.18	0.43	0.21	0.43	0.21

capture processes with rate Γ_C and annihilation processes with rate Γ_A are in equilibrium, such that $\Gamma_C = 2\Gamma_A$.

Neutrino detectors search for the charged leptons which are created by incoming neutrinos through a charged-current interaction. For the IC/DC detector we divide the muon events into *upward* events (due to upward going neutrinos interacting outside the detector volume) and *contained* events (due to neutrinos that interact within the instrumented volume); see Refs. [13,14] for details.

For both types of events, the rate depends on dark matter interactions only through Γ_C, and the choice of annihilation channel. The experimental sensitivity reflects the capture rate necessary for IC/DC to distinguish the neutrino flux due to dark matter annihilation from the atmospheric neutrino background. The capture rate is proportional to the dark matter–nucleon scattering cross section [15], so we may parameterize the capture rate by a *capture coefficient* C_0. If dark matter–nucleon scattering is spin-dependent, the capture coefficient is given by

$$\Gamma_C^{\mathrm{SD}}(m_X) = \sigma_{\mathrm{SD}}^p \times C_0^{\mathrm{SD}}(m_X). \tag{1}$$

On the other hand, if dark matter–nucleon scattering is spin-independent, then the effect of coherent scattering against heavy solar nuclei depends non-trivially on the relative strength of the dark matter couplings to neutrons and protons, f_n and f_p, respectively. Then,

$$\Gamma_C^{\mathrm{SI}}(m_X) = \sigma_{\mathrm{SI}}^p \times C_0^{\mathrm{SI}}(m_X, f_n/f_p). \tag{2}$$

The background event rate determines the dark matter-initiated charged lepton event rate Γ_{event} to which the detector is sensitive. This in turn implies that the detector has sensitivity to $\sigma_{\mathrm{SI}}^p > \sigma_{\mathrm{SI}}^{p(limit)} = \Gamma_{event}/C_0(m_X, f_n/f_p)$. We calculate C_0 using DarkSUSY [16] assuming a local halo density $\rho = 0.3$ GeV/cm^3 and a Maxwellian velocity distribution with dispersion $\bar{v} = 270$ km/s; see Appendix A.

IC/DC reports its sensitivity to the spin-dependent scattering cross section σ_{SD}^p. From this, one can easily determine IC/DC's sensitivity to σ_{SI}^p for any choice of f_n/f_p simply by rescaling the projected limit by an appropriate ratio of capture coefficients:

$$\sigma_{\mathrm{SI}}^{p(limit)} = \sigma_{\mathrm{SD}}^{p(limit)} \times \frac{C_0^{\mathrm{SD}}(m_X)}{C_0^{\mathrm{SI}}(m_X, f_n/f_p)}. \tag{3}$$

The IceCube Collaboration has recently presented an updated estimate for the sensitivity of the completed IC/DC configuration to σ_{SD}^p with 180 live days of data. This estimate assumes dark matter annihilation to the "hard" channel, that is, to $\tau\bar{\tau}$ for $m_X \leqslant 80$ GeV and to W^+W^- for $m_X > 80$ GeV. The choice of annihilation channel affects the neutrino spectrum, which in turn affects the muon event rate, and thus the detector's sensitivity.

A more conservative assumption would be dark matter annihilation to $b\bar{b}$, which is referred to as the "soft" channel. The relative sensitivity in the soft channel can be obtained by determining the ratio of muon rates at the detector (assuming a fixed dark matter–nucleon scattering cross-section) from different annihilation channels. This procedure is a valid approximation when the dark matter mass is much larger than the detector threshold since the dependence on the shapes of the neutrino spectra is weakened by integrating over a wide energy range. For dark matter masses close to the detector threshold, our results should be viewed as simply indicative of the relative sensitivities. The ratio of sensitivities for the $\tau^+\tau^-$, W^+W^- and $b\bar{b}$ channels (for various m_X) are given in Table 1.

2.1. IVDM

It is often assumed that dark matter couples identically to protons and neutrons. Under this assumption, dark matter will scatter coherently off nucleons in a nucleus, leading to an A^2 enhancement in the scattering cross section for heavy nuclei. This enhancement is the reason why the solar spin-independent capture rate is dominated by heavier nuclei, even though the Sun is largely composed of hydrogen [15]. While this assumption of isospin-conserving interactions is a valid approximation for neutralinos, it need not be true more generally.

Although isospin-violating dark matter [4,5] has been used as an explanation of the DAMA and CoGeNT data, it is really a more general scenario in which dark matter couples differently to protons than to neutrons. The dark matter–nucleus spin-independent scattering cross section is given by

$$\sigma_A \propto \mu_A^2\big[f_p Z + f_n(A-Z)\big]^2, \tag{4}$$

where μ_A is the reduced mass of the dark matter–nucleus system. The non-trivial dependence of σ_A on f_n/f_p is the reason for the dependence of $C_0^{\rm SI}$ on f_n/f_p.

3. IceCube/DeepCore versus direct detection experiments

The assumption of isospin-conserving interactions *i.e.*, $f_n = f_p$, is commonly made in normalizing the dark matter–nucleus scattering cross section for a nucleus with Z protons to that of dark matter scattering against a single nucleon. This normalized cross section σ_N^Z is given by [5]

$$\sigma_N^Z = \sigma_{\rm SI}^p \frac{\sum_i \eta_i \mu_{A_i}^2 [Z + (A_i - Z) f_n/f_p]^2}{\sum_i \eta_i \mu_{A_i}^2 A_i^2}, \tag{5}$$

where $\sigma_{\rm SI}^p$ is the spin-independent cross section for dark matter to scatter off a single proton. The summation is over the different isotopes with atomic number Z, and η_i is the natural abundance of each isotope. As expected, $\sigma_N^Z = \sigma_{\rm SI}^p$ if $f_n = f_p$, but more generally one can have $\sigma_N^Z \ll \sigma_{\rm SI}^p$.

Direct detection experiments typically report their signals or exclusion bounds in terms of σ_N^Z. But in the case of IVDM, it becomes necessary to compare the results of different experiments in terms of $\sigma_{\rm SI}^p$. It is thus useful to define the ratio [5]

$$F_Z \equiv \frac{\sigma_{\rm SI}^p}{\sigma_N^Z} = \frac{\sum_i \eta_i \mu_{A_i}^2 A_i^2}{\sum_i \eta_i \mu_{A_i}^2 [Z + (A_i - Z) f_n/f_p]^2}. \tag{6}$$

We may also define the quantity

$$F_\odot(m_X, f_n/f_p) = \frac{C_0(m_X, f_n/f_p = 1)}{C_0(m_X, f_n/f_p)}, \tag{7}$$

which, in analogy to F_Z, is the factor by which a neutrino detector's sensitivity will be suppressed if dark matter interactions violate isospin. In particular, if $\sigma_{\rm SI}^p$ is the actual dark matter–proton spin-independent scattering cross section, then $\sigma_N^\odot = \sigma_{\rm SI}^p / F_\odot$ is the "normalized to nucleon" scattering cross section which would be inferred from neutrino detector data, if one assumes isospin-conserving interactions.

We can define the quantity $R[\odot, Z](m_X, f_n/f_p)$:

$$\begin{aligned} R[\odot, Z](m_X, f_n/f_p) &\equiv \frac{\sigma_N^\odot}{\sigma_N^Z} = \frac{F_Z(f_n/f_p)}{F_\odot(m_X, f_n/f_p)} \\ &\equiv \big[R[Z, \odot](m_X, f_n/f_p)\big]^{-1}. \end{aligned} \tag{8}$$

For a fixed m_X, the maximum of $R[\odot, Z]$ (varying over f_n/f_p) is the maximum factor by which a detector with atomic number Z must exclude a signal from a neutrino detector (assuming isospin conservation) such that the signal is still excluded even if isospin violation is allowed. Similarly, the minimum of $R[\odot, Z]$ (equivalently, the maximum of $R[Z, \odot]$) is the maximum factor by which a neutrino detector must exclude a signal from a detector with atomic number Z (assuming isospin conservation) such that the signal is still excluded even if isospin violation is allowed. Table 2 shows $R_{\rm max}[\odot, Z]$ for various choices of commonly used detector elements, and various choices of m_X, while Table 3 shows $R_{\rm max}[Z, \odot]$. Note that, for elements with only one isotope, $R_{\rm max}[\odot, Z] = \infty$, since the detector will be completely insensitive to models with $f_n/f_p = -Z/(A - Z)$. We do not list these columns in Table 2.

Table 2
$R_{\rm max}[\odot, Z](f_n/f_p)$ for various elements (obtained by maximizing $R[\odot, Z](f_n/f_p)$ over $-1 \leqslant f_n/f_p \leqslant 1$).

m_X (GeV)	Xe	Ge	Si	Ca	W	Ne	C
10	281	71.2	83.4	80.1	1260	20.2	211
20	218	49.3	45.2	43.2	1000	10.8	114
30	198	42.2	33.1	31.5	920	7.82	83.4
40	188	39.0	27.1	25.6	882	6.37	68.3
50	183	37.2	23.5	22.1	861	5.51	59.4
60	179	35.7	21.0	19.7	842	4.92	53.1
70	176	34.7	19.2	18.0	830	4.50	48.7
80	173	34.0	17.9	16.8	822	4.19	45.4
90	172	33.4	16.9	15.8	815	3.95	42.9
100	170	33.0	16.1	15.0	809	3.76	40.9
200	163	30.9	12.5	11.6	782	2.92	32.0
300	161	30.2	11.5	10.5	772	2.66	29.3
400	159	29.8	10.9	10.0	767	2.54	28.0
500	159	29.6	10.7	9.76	764	2.47	27.3
600	158	29.4	10.5	9.59	762	2.43	26.9
700	158	29.3	10.4	9.47	760	2.40	26.6
800	157	29.3	10.3	9.39	759	2.37	26.4
900	157	29.2	10.2	9.33	758	2.36	26.2
1000	157	29.2	10.2	9.28	757	2.35	26.1
2000	156	29.0	9.95	9.07	754	2.29	25.6
3000	156	28.9	9.89	9.01	753	2.28	25.5
4000	156	28.9	9.86	8.98	753	2.27	25.4
5000	156	28.9	9.84	8.96	753	2.26	25.4

Table 3
$R_{\rm max}[Z, \odot](f_n/f_p)$ for various elements (obtained by maximizing $R[Z, \odot](f_n/f_p)$ over $-1 \leqslant f_n/f_p \leqslant 1$).

m_X (GeV)	Xe	Ge	Si	Ca	W	Ne	C	I	Cs	O	Na	Ar	F
10	1.87	1.00	1.00	1.00	2.23	1.00	1.00	1.60	1.75	1.00	1.00	1.00	1.00
20	3.37	1.57	1.00	1.00	4.02	1.00	1.00	2.88	3.15	1.01	1.00	1.05	1.00
30	4.54	2.11	1.00	1.01	5.42	1.00	1.01	3.88	4.24	1.01	1.00	1.42	1.00
40	5.50	2.56	1.01	1.02	6.56	1.00	1.02	4.70	5.14	1.02	1.00	1.72	1.00
50	6.29	2.93	1.01	1.02	7.50	1.00	1.03	5.37	5.87	1.03	1.00	1.96	1.00
60	7.01	3.26	1.02	1.03	8.35	1.00	1.03	5.98	6.54	1.04	1.00	2.19	1.00
70	7.61	3.55	1.02	1.03	9.07	1.00	1.04	6.50	7.11	1.04	1.00	2.38	1.00
80	8.14	3.80	1.02	1.04	9.70	1.00	1.04	6.95	7.60	1.05	1.00	2.54	1.00
90	8.60	4.01	1.03	1.04	10.3	1.00	1.05	7.34	8.03	1.06	1.00	2.69	1.00
100	9.01	4.21	1.03	1.04	10.7	1.00	1.05	7.69	8.41	1.06	1.00	2.81	1.00
200	11.4	5.34	1.05	1.07	13.6	1.01	1.08	9.73	10.6	1.09	1.00	3.56	1.00
300	12.4	5.82	1.06	1.09	14.8	1.01	1.10	10.6	11.6	1.11	1.00	3.88	1.07
400	13.0	6.07	1.07	1.10	15.4	1.01	1.11	11.1	12.1	1.12	1.00	4.04	1.12
500	13.3	6.22	1.08	1.10	15.8	1.02	1.12	11.3	12.4	1.13	1.00	4.14	1.15
600	13.5	6.32	1.08	1.11	16.1	1.02	1.12	11.5	12.6	1.14	1.00	4.21	1.16
700	13.6	6.39	1.08	1.11	16.2	1.02	1.13	11.6	12.7	1.14	1.00	4.25	1.18
800	13.7	6.43	1.08	1.11	16.4	1.02	1.14	11.7	12.8	1.15	1.00	4.28	1.19
900	13.8	6.47	1.09	1.12	16.4	1.02	1.14	11.8	12.9	1.14	1.00	4.31	1.19
1000	13.9	6.50	1.09	1.12	16.5	1.01	1.14	11.8	12.9	1.16	1.00	4.33	1.20
2000	14.2	6.63	1.09	1.14	16.8	1.03	1.16	12.0	13.2	1.17	1.00	4.41	1.22
3000	14.2	6.66	1.10	1.14	16.9	1.03	1.16	12.1	13.2	1.18	1.00	4.43	1.23
4000	14.3	6.68	1.10	1.15	17.0	1.03	1.16	12.1	13.3	1.18	1.00	4.44	1.23
5000	14.3	6.69	1.10	1.13	17.0	1.03	1.17	12.2	13.3	1.18	1.00	4.45	1.23

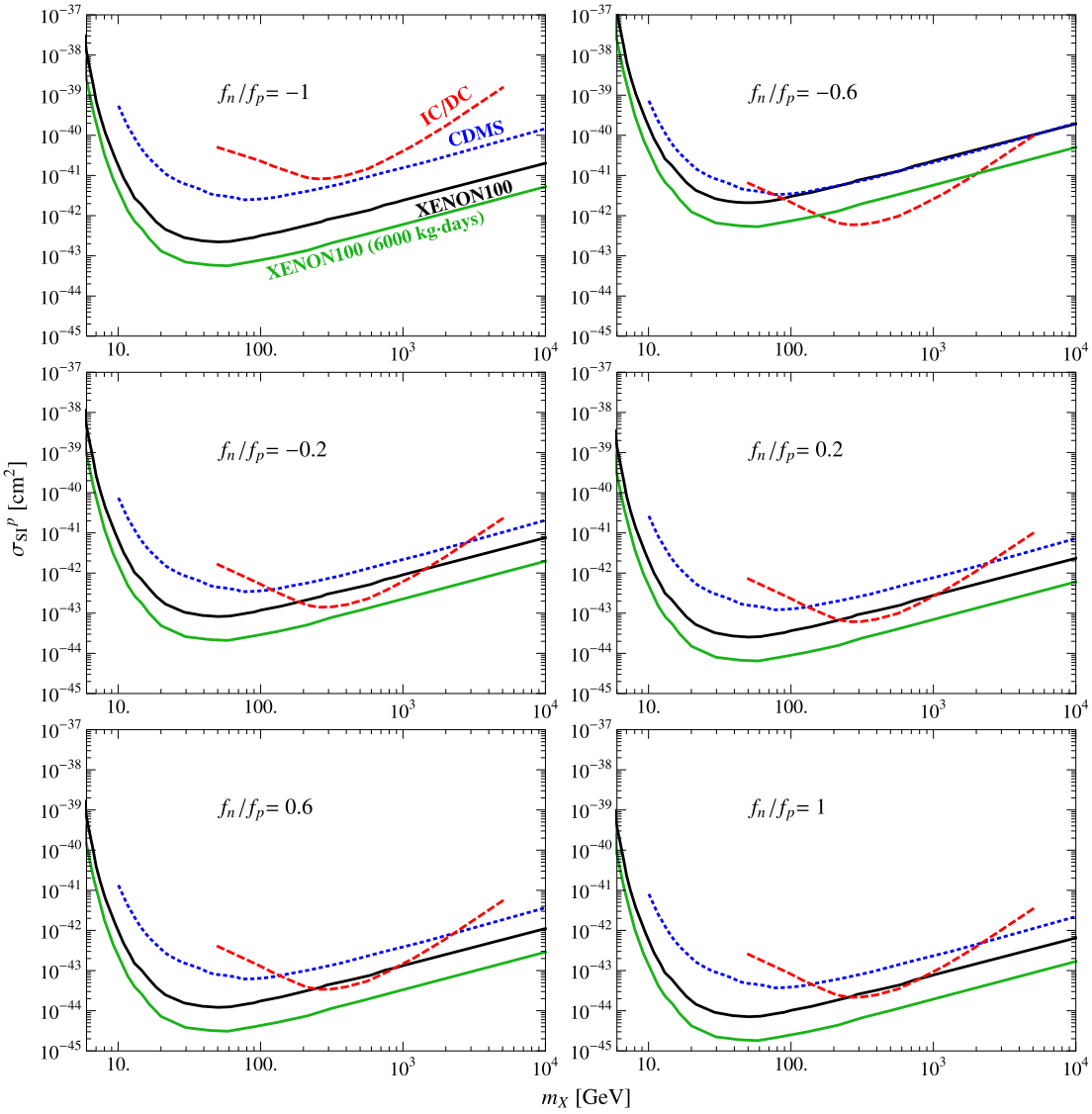

Fig. 1. Experimental sensitivity to σ_{SI}^p for various choices of f_n/f_p, as a function of dark matter mass m_X. Current limits from CDMS-II [18] (blue) and XENON100 [10] (black), expected sensitivity for XENON100 [19] (green), and IceCube (80 strings) with the DeepCore extension (6 strings) in the hard channel (red), are shown. The hard channel is annihilation to $\tau\bar{\tau}$ for $m_X < 80$ GeV, and annihilation to W^+W^- for $m_X \geqslant 80$ GeV. (For interpretation of the references to color in this figure legend, the reader is referred to the web version of this Letter.)

As is evident from Table 2, isospin violation can cause direct detection experiments to be significantly disadvantaged, relative to neutrino detectors. This effect can be particularly dramatic for direct detection experiments using heavy nuclei, such as xenon or tungsten. Since heavy atoms tend to have many more neutrons than protons, partial destructive interference between neutron and proton interactions can strikingly reduce their sensitivity. Partial destructive interference has less of an effect on nuclei such as carbon, nitrogen and oxygen, which dominate the solar capture rate, and has no effect at all on hydrogen.

On the other hand, from Table 3 we see that neutrino detectors can never be disadvantaged by isospin violation (relative to other direct detection experiments) by more than a factor of ~ 17 within the mass range considered. This "worst-case scenario" occurs when there is almost complete destructive interference ($f_n = -f_p$) in the limit of large dark matter mass (when dark matter capture through scattering off hydrogen is very inefficient). In this case, the detectors which benefit the most relative to neutrino detectors are the ones with large atomic number (and thus a mismatch between the number of protons and neutrons).

Using Eq. (3), one can rescale a neutrino detector's reported sensitivity to σ_{SD}^p for any annihilation channel, and determine its sensitivity to σ_{SI}^p for any choice of f_n/f_p and the same annihilation channel. Using Eq. (6), one can rescale the sensitivity to σ_N^Z reported by a direct detection experiment, and obtain its actual sensitivity to σ_{SI}^p for any choice of f_n/f_p. In Fig. 1, we plot IC/DC's sensitivity (in the hard channel) to σ_{SI}^p for a variety of choices of f_n/f_p, assuming 180 live days of data. (In our figures, all curves are at the 90% C.L.) We also plot the CDMS-II bound, the current bound from XENON100, and the expected sensitivity of XENON100 with 6000 kg · days exposure. In the case of isospin-conserving interactions ($f_n/f_p = 1$), IC/DC's reach is comparable with that of XENON100 in the range 260 GeV $\lesssim m_X \lesssim$ 800 GeV. For complete destructive interference ($f_n/f_p = -1$), current bounds are stronger than what IC/DC can achieve over the entire mass range considered. However, for $m_X \sim 400$ GeV ($m_X \sim 1000$ GeV), the 180-day sensitivity of IC/DC will exceed current XENON100 bounds for $-0.84 \lesssim f_n/f_p \lesssim 1$ ($-0.82 \lesssim f_n/f_p \lesssim 0.28$). Moreover, for $m_X \sim 100$ GeV, the sensitivity of IC/DC will exceed current CDMS

bounds for $-0.87 \lesssim f_n/f_p \lesssim -0.46$. We thus see that for wide ranges of m_X and f_n/f_p, IC/DC's sensitivity with 180 days of data (assuming hard channel annihilation) will exceed current bounds on dark matter–nucleon spin-independent scattering. Note that for $f_n/f_p = -0.7$ (the value for which the sensitivity of a xenon detector is maximally suppressed by isospin violation), the sensitivity of IC/DC exceeds current bounds as well as the expected sensitivity of XENON100 over the 50–5000 GeV mass range; see Fig. 2.

In Fig. 3, we show IC/DC's estimated sensitivity with 180 days of data compared to the projected sensitivity of several future experiments, such as XENON1T, SuperCDMS, MiniCLEAN, DEAP-3600 and CLEAN (using both neon and depleted argon). We plot these for $f_n/f_p = 1, -0.7, -0.82$. $f_n/f_p = -0.82$ is the value for which an argon detector's sensitivity is maximally suppressed. IC/DC with 1800 days of data will have roughly three times the sensitivity estimated with 180 days of data.

We see that for some ranges of f_n/f_p, IC/DC will be competitive with XENON1T, DEAP-3600 and CLEAN (depleted Ar). However, CLEAN (Ne) typically will have better sensitivity than IC/DC can achieve. This result is not unexpected, as neon has about as many neutrons as protons, and thus a neutrino detector will see very little relative gain in sensitivity compared to a neon detector; see Table 2.

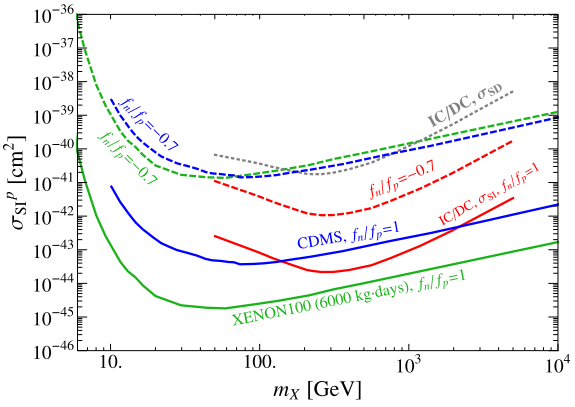

Fig. 2. Similar to Fig. 1, for $f_n/f_p = -0.7$ (dashed curves), including current bounds from CDMS-II (blue) and the expected sensitivity for XENON100 (green) and IC/DC (red). Solid curves show the isospin-conserving ($f_n/f_p = 1$) bounds and sensitivities for comparison. The gray dotted curve is the expected IC/DC sensitivity to σ_{SD} for the hard channel, which is translated into a σ_{SI}^p sensitivity by assuming all captures are due to SI scattering. (For interpretation of the references to color in this figure legend, the reader is referred to the web version of this Letter.)

4. Conclusions

We studied the prospects for spin-independent isospin-violating dark matter–nucleon scattering searches at neutrino detectors, with a focus on IceCube/DeepCore using the latest estimates of its sensitivity.

We found that isospin violation can have a very dramatic effect on the sensitivity of neutrino detectors relative to direct detection experiments. The "worst-case scenario" for neutrino detectors is complete destructive interference between proton and neutron interactions. But even in this case, neutrino detectors cannot be disadvantaged by more than a factor ~ 17. On the other hand, isospin violation can disadvantage direct detection experiments relative to neutrino experiments by up to three orders of magnitude. This difference is largely due to the many different nuclei in the Sun, including the presence of hydrogen, which is immune to the effects of destructive interference.

We plotted the expected limits from IC/DC (assuming that dark matter annihilates to the "hard" channel) and XENON100 and current limits from CDMS-II and XENON100 to σ_{SI}^p, for a variety of choices of f_n/f_p. For the standard assumption of isospin-conserving interactions, IC/DC's projected sensitivity after 180 live days is comparable with that of other detectors in the mass range 260 GeV $\lesssim m_X \lesssim$ 800 GeV. For complete destructive interference $f_n/f_p = -1$, current bounds exceed IC/DC's sensitivity. But the most optimistic scenario for the relative sensitivity of a neutrino detector is for $f_n/f_p \sim -0.7$; for this scenario, IC/DC's sensitivity exceeds that of XENON100 over the entire 50–5000 GeV range. It thus appears that for this class of IVDM models, IC/DC may indeed provide the best current prospect for dark matter detection for a wide range of parameters.

We also compared IC/DC's detection prospects with 180 days of data (its sensitivity improves by ~ 3 with 1800 days of data) to that possible with upcoming direct detection experiments, like XENON1T, SuperCDMS, and the CLEAN family of neon/argon detectors. Although IC/DC would not be able to compete with a neon-based CLEAN detector, it could (depending on the nature of isospin violation) provide sensitivity competitive with the next generation of argon, germanium and xenon-based detectors.

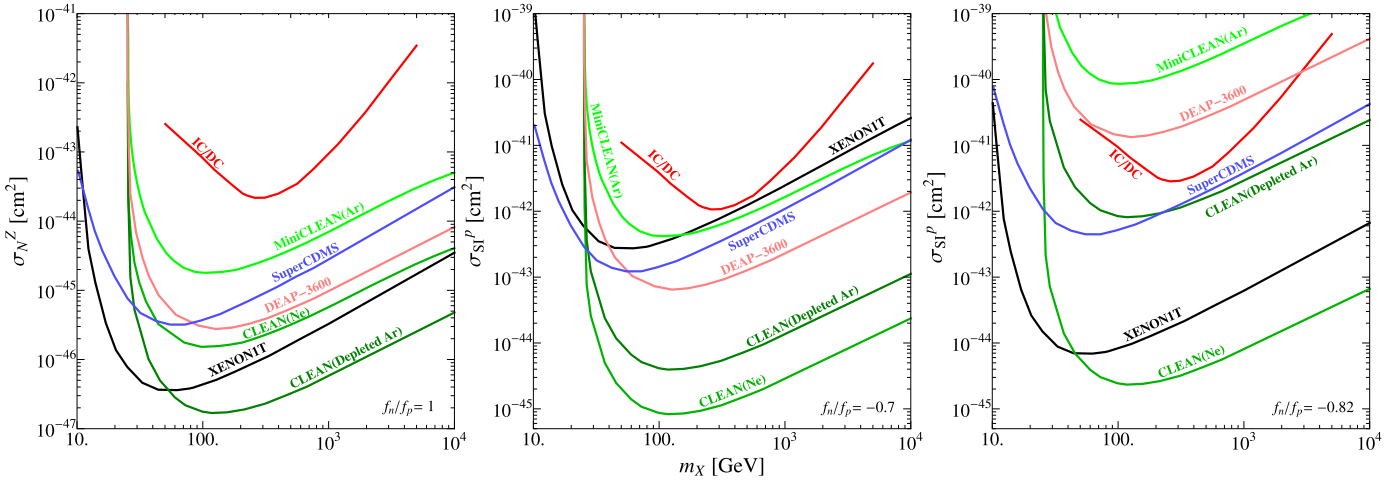

Fig. 3. Experimental sensitivity to σ_{SI}^p for $f_n/f_p = 1$ (left panel), $f_n/f_p = -0.7$ (center panel) and $f_n/f_p = -0.82$ (right panel). In addition to the expected sensitivity of IC/DC with 180 days of data we also plot prospective bounds from XENON1T [19], SuperCDMS (with a 100 kg target mass) [20], MiniCLEAN, DEAP-3600, CLEAN (Ne) and CLEAN (depleted Ar) [21] as labelled. IC/DC's sensitivity with 1800 days of data will be roughly three times better than that with 180 days of data.

Table 4
Capture coefficient $C_0^{\rm SI}(m_X, f_n/f_p)$ in units of 10^{29} s^{-1} pb^{-1}.

m_X (GeV)	$\frac{f_n}{f_p}=-1$	-0.8	-0.7	-0.6	-0.4	-0.2	0	0.2	0.4	0.6	0.8	1
10	0.10	0.14	0.21	0.30	0.58	0.98	1.5	2.1	2.9	3.8	4.7	5.9
20	0.043	0.074	0.12	0.20	0.41	0.72	1.1	1.6	2.2	2.9	3.7	4.5
30	0.025	0.048	0.087	0.14	0.31	0.55	0.86	1.2	1.7	2.2	2.8	3.5
40	0.016	0.035	0.066	0.11	0.25	0.44	0.68	0.99	1.4	1.8	2.3	2.8
50	0.012	0.027	0.053	0.090	0.20	0.36	0.56	0.81	1.1	1.5	1.8	2.3
60	8.8×10^{-3}	0.022	0.043	0.074	0.17	0.30	0.47	0.68	0.93	1.2	1.5	1.9
70	6.9×10^{-3}	0.018	0.036	0.063	0.14	0.25	0.40	0.58	0.79	1.0	1.3	1.6
80	5.6×10^{-3}	0.015	0.031	0.054	0.12	0.22	0.35	0.50	0.69	0.90	1.1	1.4
90	4.6×10^{-3}	0.013	0.027	0.047	0.11	0.19	0.30	0.44	0.60	0.79	1.0	1.2
100	3.9×10^{-3}	0.011	0.024	0.042	0.095	0.17	0.27	0.39	0.54	0.70	0.89	1.1
200	1.3×10^{-3}	4.4×10^{-3}	9.6×10^{-3}	0.017	0.039	0.071	0.11	0.16	0.22	0.29	0.37	0.46
300	6.7×10^{-4}	2.4×10^{-3}	5.3×10^{-3}	9.6×10^{-3}	0.022	0.040	0.063	0.092	0.13	0.17	0.21	0.26
400	4.2×10^{-4}	1.5×10^{-3}	3.4×10^{-3}	6.1×10^{-3}	0.014	0.026	0.041	0.059	0.081	0.11	0.14	0.17
500	2.8×10^{-4}	1.1×10^{-3}	2.4×10^{-3}	4.3×10^{-3}	9.9×10^{-3}	0.018	0.029	0.042	0.057	0.075	0.095	0.12
600	2.1×10^{-4}	7.8×10^{-4}	1.7×10^{-3}	3.1×10^{-3}	7.3×10^{-3}	0.013	0.021	0.031	0.042	0.055	0.070	0.087
700	1.6×10^{-4}	5.9×10^{-4}	1.3×10^{-3}	2.4×10^{-3}	5.6×10^{-3}	0.010	0.016	0.024	0.032	0.042	0.054	0.067
800	1.2×10^{-4}	4.7×10^{-4}	1.1×10^{-3}	1.9×10^{-3}	4.5×10^{-3}	8.1×10^{-3}	0.013	0.019	0.026	0.034	0.043	0.053
900	10×10^{-5}	3.8×10^{-4}	8.5×10^{-4}	1.6×10^{-3}	3.6×10^{-3}	6.6×10^{-3}	0.010	0.015	0.021	0.027	0.035	0.043
1000	8.2×10^{-5}	3.1×10^{-4}	7.1×10^{-4}	1.3×10^{-3}	3.0×10^{-3}	5.4×10^{-3}	8.6×10^{-3}	0.013	0.017	0.023	0.029	0.036
2000	2.2×10^{-5}	8.6×10^{-5}	1.9×10^{-4}	3.5×10^{-4}	8.2×10^{-4}	1.5×10^{-3}	2.4×10^{-3}	3.4×10^{-3}	4.7×10^{-3}	6.2×10^{-3}	7.9×10^{-3}	9.8×10^{-3}
3000	1.0×10^{-5}	3.9×10^{-5}	8.9×10^{-5}	1.6×10^{-4}	3.8×10^{-4}	6.8×10^{-4}	1.1×10^{-3}	1.6×10^{-3}	2.2×10^{-3}	2.8×10^{-3}	3.6×10^{-3}	4.5×10^{-3}
4000	5.8×10^{-6}	2.2×10^{-5}	5.1×10^{-5}	9.2×10^{-5}	2.1×10^{-4}	3.9×10^{-4}	6.2×10^{-4}	9.0×10^{-4}	1.2×10^{-3}	1.6×10^{-3}	2.1×10^{-3}	2.6×10^{-3}
5000	3.7×10^{-6}	1.4×10^{-5}	3.3×10^{-5}	5.9×10^{-5}	1.4×10^{-4}	2.5×10^{-4}	4.0×10^{-4}	5.8×10^{-4}	8.0×10^{-4}	1.1×10^{-3}	1.3×10^{-3}	1.7×10^{-3}

Table 5
$\tilde{C}_0^{\rm SI}(m_X, f_p/f_n)$ in units of 10^{29} s^{-1} pb^{-1}. In comparison to Table 4, the contribution of hydrogen to the capture rate is decreased, while heavy elements receive an enhancement due to the larger number of neutrons.

m_X (GeV)	$\frac{f_p}{f_n}=-1$	-0.8	-0.7	-0.6	-0.4	-0.2	0	0.2	0.4	0.6	0.8	1
10	0.10	0.14	0.20	0.29	0.57	0.96	1.5	2.1	2.9	3.7	4.7	5.9
20	0.043	0.086	0.14	0.22	0.44	0.75	1.2	1.7	2.2	2.9	3.7	4.5
30	0.025	0.061	0.11	0.17	0.34	0.59	0.90	1.3	1.7	2.3	2.8	3.5
40	0.016	0.047	0.083	0.13	0.27	0.47	0.72	1.0	1.4	1.8	2.3	2.8
50	0.012	0.038	0.067	0.11	0.22	0.38	0.59	0.84	1.1	1.5	1.9	2.3
60	8.8×10^{-3}	0.031	0.056	0.090	0.19	0.32	0.49	0.70	0.95	1.2	1.6	1.9
70	6.9×10^{-3}	0.026	0.047	0.077	0.16	0.27	0.42	0.60	0.81	1.1	1.3	1.6
80	5.6×10^{-3}	0.022	0.041	0.067	0.14	0.24	0.37	0.52	0.70	0.91	1.2	1.4
90	4.6×10^{-3}	0.019	0.036	0.058	0.12	0.21	0.32	0.46	0.62	0.80	1.0	1.2
100	3.9×10^{-3}	0.017	0.032	0.052	0.11	0.19	0.29	0.41	0.55	0.71	0.90	1.1
200	1.3×10^{-3}	7.0×10^{-3}	0.013	0.022	0.045	0.078	0.12	0.17	0.23	0.30	0.38	0.46
300	6.7×10^{-4}	3.9×10^{-3}	7.4×10^{-3}	0.012	0.026	0.044	0.068	0.096	0.13	0.17	0.21	0.26
400	4.2×10^{-4}	2.5×10^{-3}	4.8×10^{-3}	7.9×10^{-3}	0.017	0.028	0.044	0.062	0.084	0.11	0.14	0.17
500	2.8×10^{-4}	1.8×10^{-3}	3.4×10^{-3}	5.5×10^{-3}	0.012	0.020	0.031	0.043	0.059	0.076	0.096	0.12
600	2.1×10^{-4}	1.3×10^{-3}	2.5×10^{-3}	4.1×10^{-3}	8.5×10^{-3}	0.015	0.023	0.032	0.043	0.056	0.071	0.087
700	1.6×10^{-4}	10×10^{-4}	1.9×10^{-3}	3.1×10^{-3}	6.6×10^{-3}	0.011	0.017	0.025	0.033	0.043	0.054	0.067
800	1.2×10^{-4}	7.9×10^{-4}	1.5×10^{-3}	2.5×10^{-3}	5.2×10^{-3}	8.9×10^{-3}	0.014	0.020	0.026	0.034	0.043	0.053
900	10×10^{-5}	6.4×10^{-4}	1.2×10^{-3}	2.0×10^{-3}	4.2×10^{-3}	7.3×10^{-3}	0.011	0.016	0.021	0.028	0.035	0.043
1000	8.2×10^{-5}	5.3×10^{-4}	1.0×10^{-3}	1.7×10^{-3}	3.5×10^{-3}	6.0×10^{-3}	9.2×10^{-3}	0.013	0.018	0.023	0.029	0.036
2000	2.2×10^{-5}	1.5×10^{-4}	2.8×10^{-4}	4.6×10^{-4}	9.6×10^{-4}	1.7×10^{-3}	2.5×10^{-3}	3.6×10^{-3}	4.9×10^{-3}	6.3×10^{-3}	8.0×10^{-3}	9.8×10^{-3}
3000	1.0×10^{-5}	6.7×10^{-5}	1.3×10^{-4}	2.1×10^{-4}	4.4×10^{-4}	7.6×10^{-4}	1.2×10^{-3}	1.7×10^{-3}	2.2×10^{-3}	2.9×10^{-3}	3.6×10^{-3}	4.5×10^{-3}
4000	5.8×10^{-6}	3.8×10^{-5}	7.3×10^{-5}	1.2×10^{-4}	2.5×10^{-4}	4.3×10^{-4}	6.6×10^{-4}	9.5×10^{-4}	1.3×10^{-3}	1.7×10^{-3}	2.1×10^{-3}	2.6×10^{-3}
5000	3.7×10^{-6}	2.5×10^{-5}	4.7×10^{-5}	7.8×10^{-5}	1.6×10^{-4}	2.8×10^{-4}	4.3×10^{-4}	6.1×10^{-4}	8.2×10^{-4}	1.1×10^{-3}	1.3×10^{-3}	1.7×10^{-3}

Table 6
Capture coefficient $C_0^{\rm SD}(m_X)$ in units of 10^{29} s^{-1} pb^{-1}.

m_X (GeV)	$C_0^{\rm SD}$
10	0.094
20	0.038
30	0.021
40	0.013
50	8.7×10^{-3}
60	6.3×10^{-3}
70	4.8×10^{-3}
80	3.8×10^{-3}
90	3.0×10^{-3}
100	2.5×10^{-3}
200	6.6×10^{-4}
300	3.0×10^{-4}
400	1.7×10^{-4}
500	1.1×10^{-4}
600	7.6×10^{-5}
700	5.6×10^{-5}
800	4.3×10^{-5}
900	3.4×10^{-5}
1000	2.7×10^{-5}
2000	6.9×10^{-6}
3000	3.1×10^{-6}
4000	1.7×10^{-6}
5000	1.1×10^{-6}

Acknowledgements

We thank D. Grant, K. Richardson, C. Rott, M. Sakai and S. Smith for useful discussions. D.M. thanks the KEK Theory Center for its hospitality during the completion of this work. This research was supported in part by DOE grants DE-FG02-04ER41291, DE-FG02-04ER41308 and DE-FG02-96ER40969, and by NSF grant PHY-0544278.

Appendix A. Capture coefficients

In Table 4 we present $C_0^{\rm SI}(m_X, f_n/f_p) = \Gamma_C^{\rm SI}(m_X, f_n/f_p)/\sigma_{\rm SI}^p$ for several values of f_n/f_p between -1 and 1. For values of f_n/f_p outside this range, we instead define $\tilde{C}_0^{\rm SI}(m_X, f_p/f_n) \equiv \Gamma_C^{\rm SI}(m_X, f_n/f_p)/\sigma_{\rm SI}^n = C_0^{\rm SI}(m_X, f_n/f_p) \times (\sigma_{\rm SI}^p/\sigma_{\rm SI}^n)$. Table 5 presents $\tilde{C}_0$ in the range $-1 \leqslant f_p/f_n \leqslant 1$. Finally, in Table 6 we present $C_0^{\rm SD}(m_X) = \Gamma_C^{\rm SD}(m_X)/\sigma_{\rm SD}^p$.

References

[1] C.d.l. Heros, for the IceCube Collaboration, arXiv:1012.0184 [astro-ph.HE].
[2] J. Braun, D. Hubert, for the IceCube Collaboration, arXiv:0906.1615 [astro-ph.HE].
[3] G. Wikstrom, J. Edsjo, JCAP 0904 (2009) 009, arXiv:0903.2986 [astro-ph.CO].
[4] A. Kurylov, M. Kamionkowski, Phys. Rev. D 69 (2004) 063503, arXiv:hep-ph/0307185;
F. Giuliani, Phys. Rev. Lett. 95 (2005) 101301, arXiv:hep-ph/0504157;
S. Chang, J. Liu, A. Pierce, N. Weiner, I. Yavin, JCAP 1008 (2010) 018, arXiv:1004.0697 [hep-ph].
[5] J.L. Feng, J. Kumar, D. Marfatia, D. Sanford, arXiv:1102.4331 [hep-ph].
[6] R. Bernabei, P. Belli, F. Cappella, R. Cerulli, C.J. Dai, A. d'Angelo, H.L. He, A. Incicchitti, et al., Eur. Phys. J. C 67 (2010) 39, arXiv:1002.1028 [astro-ph.GA].
[7] C.E. Aalseth, P.S. Barbeau, J. Colaresi, J.I. Collar, J.D. Leon, J.E. Fast, N. Fields, T.W. Hossbach, et al., arXiv:1106.0650 [astro-ph.CO].
[8] See talk by W. Seidel, http://indico.in2p3.fr/contributionDisplay.py?contribId=195&sessionId=9&confId=1565.
[9] D.S. Akerib, et al., CDMS Collaboration, Phys. Rev. D 82 (2010) 122004, arXiv:1010.4290 [astro-ph.CO];
Z. Ahmed, et al., CDMS-II Collaboration, Phys. Rev. Lett. 106 (2011) 131302, arXiv:1011.2482 [astro-ph.CO];
J. Angle, et al., XENON10 Collaboration, arXiv:1104.3088 [astro-ph.CO];
T. Girard, et al., for the SIMPLE Collaboration, arXiv:1101.1885 [astro-ph.CO].
[10] E. Aprile, et al., XENON100 Collaboration, arXiv:1104.2549 [astro-ph.CO].
[11] J. Kumar, J.G. Learned, M. Sakai, S. Smith, arXiv:1103.3270 [hep-ph].
[12] S.-L. Chen, Y. Zhang, arXiv:1106.4044 [hep-ph].
[13] V. Barger, J. Kumar, D. Marfatia, E.M. Sessolo, Phys. Rev. D 81 (2010) 115010, arXiv:1004.4573 [hep-ph].
[14] V. Barger, Y. Gao, D. Marfatia, Phys. Rev. D 83 (2011) 055012, arXiv:1101.4410 [hep-ph].
[15] A. Gould, Astrophys. J. 321 (1987) 571;
G. Jungman, M. Kamionkowski, K. Griest, Phys. Rep. 267 (1996) 195, hep-ph/9506380.
[16] P. Gondolo, et al., JCAP 0407 (2004) 008, astro-ph/0406204.
[17] M.C. Gonzalez-Garcia, F. Halzen, S. Mohapatra, Astropart. Phys. 31 (2009) 437, arXiv:0902.1176 [astro-ph.HE].
[18] Z. Ahmed, et al., The CDMS-II Collaboration, Science 327 (2010) 1619, arXiv:0912.3592 [astro-ph.CO];
Z. Ahmed, et al., CDMS Collaboration, EDELWEISS Collaboration, arXiv:1105.3377 [astro-ph.CO].
[19] See talk by D. Cline, http://public.lanl.gov/friedland/info11/info11talks/ClineDM-INFO11.pdf.
[20] See talk by T. Saab, http://indico.in2p3.fr/contributionDisplay.py?sessionId=26&contribId=58&confId=1565.
[21] See talk by R. Hennings-Yeomans, http://deapclean.org/talks/PHENO2011_Hennings.pdf.